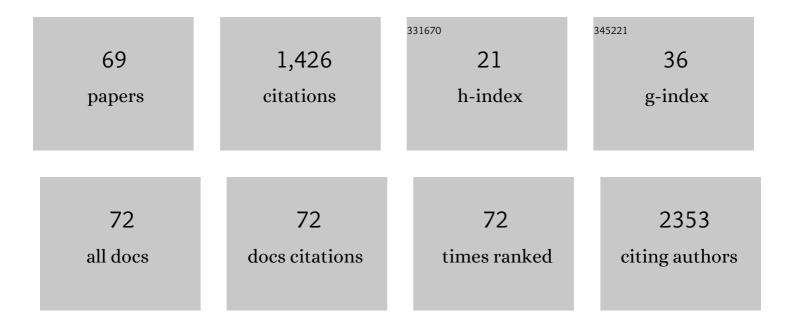


List of Publications by Year in descending order

Source: https://exaly.com/author-pdf/1839543/publications.pdf Version: 2024-02-01



I EI YU

#	Article	IF	CITATIONS
1	Adjuvant Transarterial Chemoembolization for HBV-Related Hepatocellular Carcinoma After Resection: A Randomized Controlled Study. Clinical Cancer Research, 2018, 24, 2074-2081.	7.0	181
2	Fabrication of urchin-like NiCo ₂ (CO ₃) _{1.5} (OH) ₃ @NiCo ₂ S ₄ on Ni foam by an ion-exchange route and application to asymmetrical supercapacitors. Journal of Materials Chemistry A, 2015, 3, 13308-13316.	10.3	101
3	Facile synthesis of exfoliated Co–Al LDH–carbon nanotube composites with high performance as supercapacitor electrodes. Physical Chemistry Chemical Physics, 2014, 16, 17936-17942.	2.8	92
4	Optimizing the charge transfer process by designing Co ₃ O ₄ @PPy@MnO ₂ ternary core–shell composite. Journal of Materials Chemistry A, 2014, 2, 12968-12973.	10.3	84
5	Near-Infrared Electrochemiluminescence Immunoassay with Biocompatible Au Nanoclusters as Tags. Analytical Chemistry, 2020, 92, 7581-7587.	6.5	82
6	MicroRNA-29a induces loss of 5-hydroxymethylcytosine and promotes metastasis of hepatocellular carcinoma through a TET–SOCS1–MMP9 signaling axis. Cell Death and Disease, 2017, 8, e2906-e2906.	6.3	66
7	Characterization of Fe3O4/SiO2/Gd2O(CO3)2 core/shell/shell nanoparticles as T1 and T2 dual mode MRI contrast agent. Talanta, 2015, 131, 661-665.	5.5	60
8	Facile growth of hollow porous NiO microspheres assembled from nanosheet building blocks and their high performance as a supercapacitor electrode. CrystEngComm, 2014, 16, 10389-10394.	2.6	51
9	The growth and assembly of the multidimensional hierarchical Ni ₃ S ₂ for aqueous asymmetric supercapacitors. CrystEngComm, 2015, 17, 4495-4501.	2.6	44
10	Feature extraction of wood-hole defects using wavelet-based ultrasonic testing. Journal of Forestry Research, 2017, 28, 395-402.	3.6	43
11	Biomass-derived C/N co-doped Ni(OH) ₂ /Ni _x S _y with a sandwich structure for supercapacitors. Journal of Materials Chemistry A, 2018, 6, 17417-17425.	10.3	37
12	Fe ₃ O ₄ -CoP _{<i>x</i>} Nanoflowers Vertically Grown on TiN Nanoarrays as Efficient and Stable Electrocatalysts for Overall Water Splitting. ACS Applied Nano Materials, 2019, 2, 40-47.	5.0	34
13	Facet Engineering in Ultrathin Two-Dimensional NiFe Metal–Organic Frameworks by Coordination Modulation for Enhanced Electrocatalytic Water Oxidation. ACS Sustainable Chemistry and Engineering, 2021, 9, 10892-10901.	6.7	34
14	The Preparation of Au@TiO2 Yolk–Shell Nanostructure and its Applications for Degradation and Detection of Methylene Blue. Nanoscale Research Letters, 2017, 12, 535.	5.7	33
15	A ratiometric electrochemical sensor for multiplex detection of cancer biomarkers using bismuth as an internal reference and metal sulfide nanoparticles as signal tags. Analyst, The, 2019, 144, 4073-4080.	3.5	32
16	Bovine serum albumin-stabilized silver nanoclusters with anodic electrochemiluminescence peak at 904Ânm in aqueous medium and applications in spectrum-resolved multiplexing immunoassay. Biosensors and Bioelectronics, 2021, 176, 112934.	10.1	32
17	A Simple, Rapid Method for Determination of Melatonin in Plant Tissues by UPLC Coupled with High Resolution Orbitrap Mass Spectrometry. Frontiers in Plant Science, 2017, 8, 64.	3.6	31
18	PI-88 inhibits postoperative recurrence of hepatocellular carcinoma via disrupting the surge of heparanase after liver resection. Tumor Biology, 2016, 37, 2987-2998.	1.8	29

Lei Yu

#	Article	IF	CITATIONS
19	Effect of moisture content on the ultrasonic acoustic properties of wood. Journal of Forestry Research, 2015, 26, 753-757.	3.6	28
20	The 2015–2016 Ground Displacements of the Shanghai Coastal Area Inferred from a Combined COSMO-SkyMed/Sentinel-1 DInSAR Analysis. Remote Sensing, 2017, 9, 1194.	4.0	28
21	Exosome-depleted MiR-148a-3p derived from Hepatic Stellate Cells Promotes Tumor Progression via ITGA5/PI3K/Akt Axis in Hepatocellular Carcinoma. International Journal of Biological Sciences, 2022, 18, 2249-2260.	6.4	27
22	Liquid Crystalline Nanocolloids for the Storage of Electro-Optic Responsive Images. ACS Applied Materials & Interfaces, 2019, 11, 8612-8624.	8.0	25
23	Boosting Alkaline Hydrogen Evolution on Stoichiometric Molybdenum Carbonitride via an Interstitial Vacancyâ€Elimination Strategy. Advanced Energy Materials, 2022, 12, .	19.5	21
24	Cytotoxic Triterpenoid Glycosides from the Roots of <i>Gordonia chrysandra</i> . Journal of Natural Products, 2009, 72, 866-870.	3.0	18
25	Quantifying Components of Soil Respiration and Their Response to Abiotic Factors in Two Typical Subtropical Forest Stands, Southwest China. PLoS ONE, 2015, 10, e0117490.	2.5	18
26	Applying multifractal spectrum combined with fractal discrete Brownian motion model to wood defects recognition. Wood Science and Technology, 2011, 45, 511-519.	3.2	14
27	Medical Image Edge Detection Based on Omni-directional Multi-Scale Structure Element of Mathematical Morphology. , 2007, , .		13
28	Phosphorus deficiency promotes the lateral root growth of <i>Fraxinus mandshurica</i> seedlings. Journal of Plant Nutrition and Soil Science, 2019, 182, 552-559.	1.9	12
29	Mechanical properties of wood materials using near-infrared spectroscopy based on correlation local embedding and partial least-squares. Journal of Forestry Research, 2020, 31, 1053-1060.	3.6	12
30	Effects of Hormones and Epigenetic Regulation on the Callus and Adventitious Bud Induction of Fraxinus mandshurica Rupr Forests, 2020, 11, 590.	2,1	12
31	Low-voltage-driven and highly-diffractive holographic polymer dispersed liquid crystals with spherical morphology. RSC Advances, 2017, 7, 51847-51857.	3.6	11
32	Static gesture segmentation technique based on improved Sobel operator. Journal of Engineering, 2019, 8339-8342.	1.1	10
33	A differential photoelectrochemical method for glucose determination based on alkali-soaked zeolite imidazole framework-67 as both glucose oxidase and peroxidase mimics. Mikrochimica Acta, 2020, 187, 244.	5.0	10
34	Characteristics and Expression Analysis of FmTCP15 under Abiotic Stresses and Hormones and Interact with DELLA Protein in Fraxinus mandshurica Rupr Forests, 2019, 10, 343.	2.1	9
35	Laparoscopic diverticulectomy with the aid of intraoperative gastrointestinal endoscopy to treat epiphrenic diverticulum. Journal of Minimal Access Surgery, 2016, 12, 366.	0.7	9
36	Bipolar ï€-conjugation interrupted host polymers by metal-free superacid-catalyzed polymerization for single-layer electrophosphorescent diodes. RSC Advances, 2014, 4, 50027-50034.	3.6	8

Lei Yu

#	Article	IF	CITATIONS
37	In vitro analysis of the role of the mitochondrial apoptosis pathway in CSBE therapy against human gastric cancer. Experimental and Therapeutic Medicine, 2015, 10, 2403-2409.	1.8	8
38	Propagation behavior of acoustic wave in wood. Journal of Forestry Research, 2014, 25, 671-676.	3.6	6
39	Establishment of a micropropagation supporting technology for the Fraxinus mandshurica × Fraxinus sogdiana. In Vitro Cellular and Developmental Biology - Plant, 2021, 57, 307-318.	2.1	6
40	Application of X-ray Computed Tomography to Automatic Wood Testing. , 2007, , .		5
41	Integrated Bioinformatics analysis and clinical validation reveals that high expression of mucin 1 in	1.8	5
42	Surgical Resection plus Radiofrequency Ablation versus Radical Surgery for Hepatocellular Carcinoma: A Propensity Score Matching Analysis. Journal of Cancer, 2019, 10, 3933-3940.	2.5	4
43	Multifractal spectrum theory used to medical image from CT testing. , 2008, , .		3
44	Molecular cloning and expression under abiotic stresses and hormones of the ethylene response factor VII gene FmRAP2.12 from Fraxinus mandshurica. Journal of Forestry Research, 2019, 30, 1289-1300.	3.6	3
45	Transcriptome Analysis for Fraxinus mandshurica Rupr. Seedlings from Different Carbon Sequestration Provenances in Response to Nitrogen Deficiency. Forests, 2021, 12, 257.	2.1	3
46	Automatic and Fast Testing of Wood Density Based on Computed Tomography. , 2007, , .		2
47	A detection method on wood defects of CT image using multifractal spectrum based on fractal brownian motion. , 2008, , .		2
48	Applying multifractal spectrum combined with fractal discrete brownian motion model to wood defects recognition for sawing. , 2009, , .		2
49	Study of a Prediction Model for Forest Fire-Initial Burnt Area on Meteorological Factors. , 2009, , .		2
50	CT number in wood physical properties prediction based on computed tomography technology. , 2010, ,		2
51	A D2D mode selection scheme with energy consumption minimization underlaying two-tier heterogeneous cellular networks. , 2017, , .		2
52	Variation in carbon traits among Fraxinus mandshurica populations and allometric equations between carbon traits and growth traits. New Forests, 2021, 52, 921.	1.7	2
53	Development and validation of a non-invasive model for diagnosing HBV-related liver cirrhosis. Clinica Chimica Acta, 2021, 523, 525-531.	1.1	2
54	Six statistical issues in scientific writing that might lead to rejection of a manuscript. Journal of Forestry Research, 2022, 33, 731-739.	3.6	2

Lei Yu

#	Article	IF	CITATIONS
55	Detection and Classification of Wood Defects by ANN. , 2006, , .		1
56	Improved multi-scale and structuring element morphological detection in the log CT image. , 2008, , .		1
57	Research on recognition of wood defect types based on back-propagation neural network. , 2008, , .		1
58	The application of mathematical morphological optimization algorithm in edge detection of defected wood image. , 2008, , .		1
59	Improved morphological method in the detection of log CT image with defect. , 2008, , .		1
60	Medical Image Testing Based on Fractal Spectrum Theory. , 2009, , .		1
61	Log x-ray image edge detection based on fractal-morphology analysis. , 2010, , .		1
62	Integrated Bioinformatics analysis and clinical validation reveals that high expression of mucin 1 in intrahepatic cholangiocarcinoma predicts recurrence after curative resection. Experimental and Therapeutic Medicine, 2020, 20, 50.	1.8	1
63	Based on Computed Tomography Multifractal Analysis of Wood Defect. , 2007, , .		Ο
64	Application of omnidirectional structure element of mathematical morphology to wood computed tomography testing. , 2008, , .		0
65	Omnidirectional morphology applied to wood defects testing by using computed tomography. , 2008, , .		0
66	Image edge detection of wood defects based on multi-fractal analysis. , 2008, , .		0
67	Analysis of Relationship between Apoptosis and Changes of Ca ²⁺ in HepG-2 induced by CSA with laser scanning confocal technology. , 2009, , .		0
68	Effects of Toluene Diisocyanate on Cytokine in Mice Blood Serum. International Conference on Bioinformatics and Biomedical Engineering: [proceedings] International Conference on Bioinformatics and Biomedical Engineering, 2010, , .	0.0	0
69	Runoff Fractal Dimension of Songhua River Basin in Harbin Station Based on Db4 Wavelet. Advanced Materials Research, 2012, 550-553, 2537-2540.	0.3	Ο